Langmuir
Article
pubs.acs.org/Langmuir

Directed Self-Assembly of Colloidal Dumbbells with an Electric Field

Ahmet Faik Demirörs,*[,†] Patrick M. Johnson,[‡] Carlos M. van Kats,[†] Alfons van Blaaderen,[†] and Arnout Imhof*[,†]

[†]*Soft Condensed Matter, Debye Institute for Nanomaterials Science, Department of Physics and Astronomy, Utrecht University, Princetonplein 5, 3584 CC Utrecht, The Netherlands, and* [‡]*FOM Institute for Atomic and Molecular Physics, Science Park 102, 1098 XG Amsterdam, The Netherlands*

Received May 26, 2010. Revised Manuscript Received July 21, 2010

We demonstrate the assembly of colloidal particles with the shape of diatomic molecules ("dumbbells") into crystals that we study with confocal microscopy. The literature on the preparation of nonspherical colloidal particles has grown steadily. Assembly of these particles into regular three-dimensional crystalline lattices, however, is rarely, if ever, achieved and has not yet been studied quantitatively in 3D real space. We find that, by application of an electric field, such particles assemble quite readily. By varying the particle aspect ratio, range of interactions, and electric field strength, we find several different crystal structures of which three have never before been observed. Moreover, the electric field can be used to switch between different structures and manipulate/switch the photonic properties. Moreover, our work sheds light on fundamental questions related to the self-assembly of nonspherical particles.

1. Introduction

Creating new types of colloidal crystals is vital for understanding crystallization and colloidal interactions,[1] as well as for developing advanced materials such as photonic crystals.[2] However, the range of colloidal crystals produced by common spherical colloids is limited. This range can be expanded by applying external electric fields to the dispersions[3−5] or by using colloids that have nonspherical shapes or interaction potentials.[6−10] However, what happens when external fields are applied to dispersions of nonspherical colloids? Here, we show that external electric fields applied to anisotropic colloidal silica dumbbells (dimers) lead to entirely new crystal structures and prevent arrest in a glassy state. The exact structures of these crystals, including multidomain structures, were determined in real space through the use of index matching and confocal microscopy. The effect on the phase behavior of three separate parameters, the aspect ratio (length/width), the double layer thickness relative to the particle size, and the electric field strength, was investigated. Even a sparse probing of this parameter space yielded five different crystal structures of which three have never before been observed. Moreover, one martensitic crystal−crystal transition was found as a function of the electric field strength. The properties of the low-density dumbbell crystals were also found to be tunable via the application of an external electric field which reoriented the dumbbells without destroying the crystallinity.

For our studies, we have chosen one of the simplest possible nonspherical particles, two spheres held together, which we refer to as a dumbbell. The anisotropy of such a particle can be defined by its aspect ratio, $L^* = L/\sigma$, where L is the distance between the centers of the two overlapping spheres and σ is the diameter of each sphere. Such particles are fundamentally interesting because they represent the colloidal analogue of diatomic molecules. They may also be useful as photonic band gap materials.[11] For instance, Li et al.[12] have shown theoretically that dumbbell crystals ordered in specific crystal lattices can exhibit a full photonic band gap.

The phase behavior of hard dumbbells with no external field has been simulated.[13,14] In the phase diagram of hard dumbbells, Marechal and Dijkstra observed plastic crystals for aspect ratios below 0.4. In plastic crystals, particles have positional order but no long-range orientational order. For aspect ratios over 0.4 and at higher volume fractions, they predicted an ordered crystal phase. For aspect ratios over 0.9, an aperiodic crystal phase was found in simulations. Hard and soft dumbbells in external fields have yet to be simulated.

The first experimental papers on dumbbell self-organization in the absence of external fields have been recently presented. These focused mainly on 2D structures produced by convective drying,[15,16] i.e., via a nonequilibrium process. A plastic crystal was seen in low aspect ratio ($L^* = 0.28, 0.33$) dumbbells, while an aperiodic structure formed in a system with aspect ratio close to unity. In 3D, Mock and Zukoski[17] have studied the formation of crystal structures from dumbbell-like particles with low aspect ratios ($L^* = 0.26$). They observed plastic crystals and body-centered-tetragonal *bct* crystals of aligned particles. In external fields, self-organization of dumbbell particles was investigated by

*Correspondence should be addressed to A. F. Demirörs, A.F.Demirors@uu.nl, and A.Imhof, A.Imhof@uu.nl.

(1) Palberg, T. *J. Phys.: Condens. Matter* **1999**, *11*, R323–R360.
(2) Imhof, A. Three-dimensional photonic crystals made from colloids. In *Nanoscale Materials*, Liz-Marzan, L. M., Kamat, P. V., Eds.; Kluwer Academic: Dordrecht, 2003; pp 423−454.
(3) Hoogenboom, J. P.; van Langen-Suurling, A. K.; Romijn, J.; van Blaaderen, A. *Phys. Rev. Lett.* **2003**, *90*, 138301.
(4) Dassanayake, U.; Fraden, S.; van Blaaderen, A. *J. Chem. Phys.* **2000**, *112*, 3851–3858.
(5) Hynninen, A. P.; Dijkstra, M. *Phys. Rev. Lett.* **2005**, *94*, 138303.
(6) Glotzer, S. C.; Solomon, M. J. *Nat. Mater.* **2007**, *6*, 557–562.
(7) van Blaaderen, A. *Nature* **2006**, *439*, 545–546.
(8) van Blaaderen, A.; Ruel, R.; Wiltzius, P. *Nature* **1997**, *385*, 321–324.
(9) Yethiraj, A.; van Blaaderen, A. *Nature* **2003**, *421*, 513–517.
(10) Yang, S. M.; Kim, S. H.; Lim, J. M.; Yi, G. R. *J. Mater. Chem.* **2008**, *18*, 2177–2190.
(11) Hosein, I. D.; Ghebrebrhan, M.; Joannopoulos, J. D.; Liddell, C. M. *Langmuir* **2009**, *26*, 2151–2159.
(12) Li, Z. Y.; Wang, J.; Gu, B. Y. *J. Phys. Soc. Jpn.* **1998**, *67*, 3288–3291.
(13) Vega, C.; Monson, P. A. *J. Chem. Phys.* **1997**, *107*, 2696–2697.
(14) Marechal, M.; Dijkstra, M. *Phys. Rev. E* **2008**, *77*, 10.
(15) Lee, S. H.; Gerbode, S. J.; John, B. S.; Wolfgang, A. K.; Escobedo, F. A.; Cohen, I.; Liddell, C. M. *J. Mater. Chem.* **2008**, *18*, 4912–4916.
(16) Hosein, I. D.; John, B. S.; Lee, S. H.; Escobedo, F. A.; Liddell, C. M. *J. Mater. Chem.* **2009**, *19*, 344–349.
(17) Mock, E. B.; Zukoski, C. F. *Langmuir* **2007**, *23*, 8760–8771.

Stephanie and Liddell[18] in 2D systems and of ellipsoids by Tung et al. in 3D systems by convective drying.[19]

In the experiments presented here, dumbbell crystals were obtained by sedimentation of charge-stabilized silica dumbbells in a refractive index matching solvent within the presence of an electric field. The electric field strength in the dispersion was calculated by considering the three dielectric layers between the electrodes (glass−dispersion−glass) as three capacitors connected in series (see Experimental Section). Silica dumbbell dispersions were put in a 0.2 mm × 0.2 mm square capillary with Au/Cr electrodes on two opposite sides.[20] The dumbbell particle cores were labeled and imaged with an inverted confocal microscope. Particle coordinates were tracked to find the exact structure of the crystals in real space (see Experimental Section). The field-induced crystals had an average height of 7−11 layers of particles.

2. Experimental Section

1.3 μm and 800 nm silica spheres were synthesized using seeded growth via the method of Stöber[21] with a rhodamine isothiocyanate (RITC) labeled core.[22] The dumbbells were fabricated according to the procedure of Johnson et al.[23] For the 0.9 aspect ratio dumbbells, 1.3 μm silica particles were first dimerized and then coated with a thin silica layer to covalently bind the spheres. For 0.7 aspect ratio dumbbells, 800 nm silica dimerized particles were coated with extra silica to a diameter of 1.1 μm per sphere of the dumbbell. The silica dumbbells were purified with density gradient centrifugation (DGC).[23] No more than 1% of spheres were left in the dumbbell suspension after DGC. For dispersing the silica dumbbells in relatively polar solvents like dimethylsulfoxide (DMSO), no extra treatment was necessary.

The crystal structure for hard dumbbells was annealed by flipping the sample cell up and down 3−4 times and repeating the sedimentation while keeping the field on, in a similar procedure previously used for spheres.[24]

Dispersing the particles in cyclohexyl bromide (CHB, $\varepsilon = 7.9$) required surface modification. These particles were coated with a layer of 3-(trimethoxysilyl)propyl methacrylate (TPM) under Stöber conditions prior to DGC. Following DGC, the purified dumbbells were dried and then dispersed in a CHB/polymer stabilizer solution (5−15 mg of poly(12-hydroxy stearic acid) (PHSA)-poly(methyl methacrylate) (PMMA) graft-comb stabilizer dissolved in 10 g of CHB). This stabilizer was synthesized according to the procedure of Bosma et al.[25] As described by Leunissen et al.,[26] charged particles dispersed in a solvent of dielectric constant $4 \leq \varepsilon \leq 10$ exhibit soft interactions for sufficiently low ionic strengths.

Refractive index matched DMSO/water solutions were prepared as described in ref 24, where 11.6% water was mixed with 88.4% DMSO by weight. The refractive index difference in CHB solutions was 0.05, which is low enough to allow visualization of up to 150 μm with the confocal microscope.

Confocal microscope images were taken mostly parallel with the xy image plane, which is defined to be perpendicular to gravity. A 3D crystal was scanned in sequence in the direction along the optical or z-axis to build up a z-stack. These sets of images were used to find the coordinates of dumbbells and to construct images in yz and xz planes.[4,8] For 0.9 aspect ratio dumbbells, the high aspect ratio complicates the visualization of the dumbbell particles. Only the cores of the two spheres that make up the dumbbells are visible in the microscopy image. At high aspect ratio and high dumbbell density, it is difficult to tell whether two cores belong to the same dumbbell or to two touching dumbbells in still images. This problem is solved by examining movies of the particles. In such movies, dumbbells can be recognized because the coupled centers move in unison.

The initial volume fractions of the dispersions were 7−9% for the hard dumbbells and 0.05−1% for the soft dumbbells. The initial volume fractions were kept high to create as many layers of sediment as possible in a small capillary. The lower volume fraction for the soft dumbbells was chosen because of the long interaction length of these particles.

It was not possible to density match these particles. The gravitational length of our dumbbells was 230 nm for 0.9 aspect ratio dumbbells in DMSO/water. It was 400 nm for 0.7 aspect ratio hard dumbbells in DMSO/water and 320 nm for soft dumbbells in CHB.

Particle dispersions were inserted into a capillary, similar to those described by Leunissen et al.,[20] to allow for ac electric field application. These capillaries had a 0.4 mm square outer cross section and a 0.2 mm inner cross section. Electrodes (chromium (3 nm) and gold (9 nm)) were sputter-coated onto two opposite sides of the capillary. For this construction, electric field strength was corrected for the three dielectric layers between the electrodes (glass−dispersion−glass) by considering the stack as three capacitors connected in series. The general formula for there stacks is given as follows:

$$E_i = \frac{V}{\varepsilon_i}\left(\frac{\varepsilon_1\varepsilon_2\varepsilon_3}{d_1\varepsilon_2\varepsilon_3 + d_2\varepsilon_1\varepsilon_3 + d_3\varepsilon_1\varepsilon_2}\right) \quad (1)$$

Here, V is the applied voltage, E_i is the effective electric field strength on the ith ($i = 1, 2, 3$) layer, ε_i is the dielectric constant, and d_i is the thickness of the layer. The electric field was perpendicular to the gravitational field. A frequency of 1 MHz was used for the electric field. This frequency was high enough that the double layer ions could not follow the field.

For estimating the relative strength of the electric field induced dipolar interactions for each experimental condition, we used the dimensionless prefactor γ. This parameter is defined for spheres as[27]

$$\gamma = \frac{\pi\sigma^3\beta^2\varepsilon_m\varepsilon_0|\mathbf{E}_{loc}|^2}{8k_BT} \quad (2)$$

Here, σ is the diameter of the sphere, β is the polarizability of the particles in the medium, ε_m is the dielectric constant of the medium, and $\mathbf{E}_{loc}$ is the local electric field. The polarizability of the particles in the medium is given by $\beta = (\varepsilon_p - \varepsilon_m)/(\varepsilon_p + 2\varepsilon_m)$, where ε_p is the dielectric constant of the particles. The local field is defined as $\mathbf{E}_{loc} = \mathbf{E} + \mathbf{E}_{dip}$ where $\mathbf{E}$ is the external field and $\mathbf{E}_{dip}$ is the field induced by the other dipoles. Here, $\mathbf{E}_{loc}$ was estimated by $\mathbf{E}_{loc} = \mathbf{E}/(1 - \beta\pi/6)$.[28] Detailed information about eq 2 can be found in ref 27 along with the phase diagrams of dipolar hard and soft spheres. We estimated σ as the diameter of a sphere that has half the volume of a dumbbell. To estimate the volume of the dumbbell, we used the following formula, where r is the radius of a sphere of the dumbbell:

$$V_{db} = \frac{4\pi r^3}{3}\left(1 + \frac{3}{2}L^* - \frac{1}{2}(L^*)^3\right) \quad (3)$$

We investigated the following experimental conditions: Hard dumbbells with aspect ratios 0.9 and 0.7 at a γ of 10.2 (28 V_{rms}/mm) for 0.9 and at γ of 4.0 (23 V_{rms}/mm) and 10.3 (37 V_{rms}/mm)

(18) Stephanie, H. L.; Chekesha, M. L. *Small* **2009**, *5*, 1957–1962.
(19) Tao, D.; Kai, S.; Koen, C.; Chen-Ho, T. *Adv. Mater.* **2009**, *21*, 1936–1940.
(20) Leunissen, M. E.; Vutukuri, H. R.; van Blaaderen, A. *Adv. Mater.* **2009**, *21*, 3116.
(21) Stöber, W.; Fink, A.; Bohn, E. *J. Colloid Interface Sci.* **1968**, *26*, 62–69.
(22) van Blaaderen, A.; Vrij, A. *Langmuir* **1992**, *8*, 2921–2931.
(23) Johnson, P. M.; van Kats, C. M.; van Blaaderen, A. *Langmuir* **2005**, *21*, 11510–11517.
(24) Yethiraj, A.; Thijssen, J. H. J.; Wouterse, A.; van Blaaderen, A. *Adv. Mater.* **2004**, *16*, 596–600.
(25) Bosma, G.; Pathmamanoharan, C.; de Hoog, E. H. A.; Kegel, W. K.; van Blaaderen, A.; Lekkerkerker, H. N. W. *J. Colloid Interface Sci.* **2002**, *245*, 292–300.
(26) Leunissen, M. E.; van Blaaderen, A.; Hollingsworth, A. D.; Sullivan, M. T.; Chaikin, P. M. *Proc. Natl. Acad. Sci. U.S.A.* **2007**, *104*, 2585–2590.
(27) Hynninen, A. P.; Dijkstra, M. *Phys. Rev. E* **2005**, *72*, 10.
(28) Tao, R.; Sun, J. M. *Phys. Rev. Lett.* **1991**, *67*, 398–401.

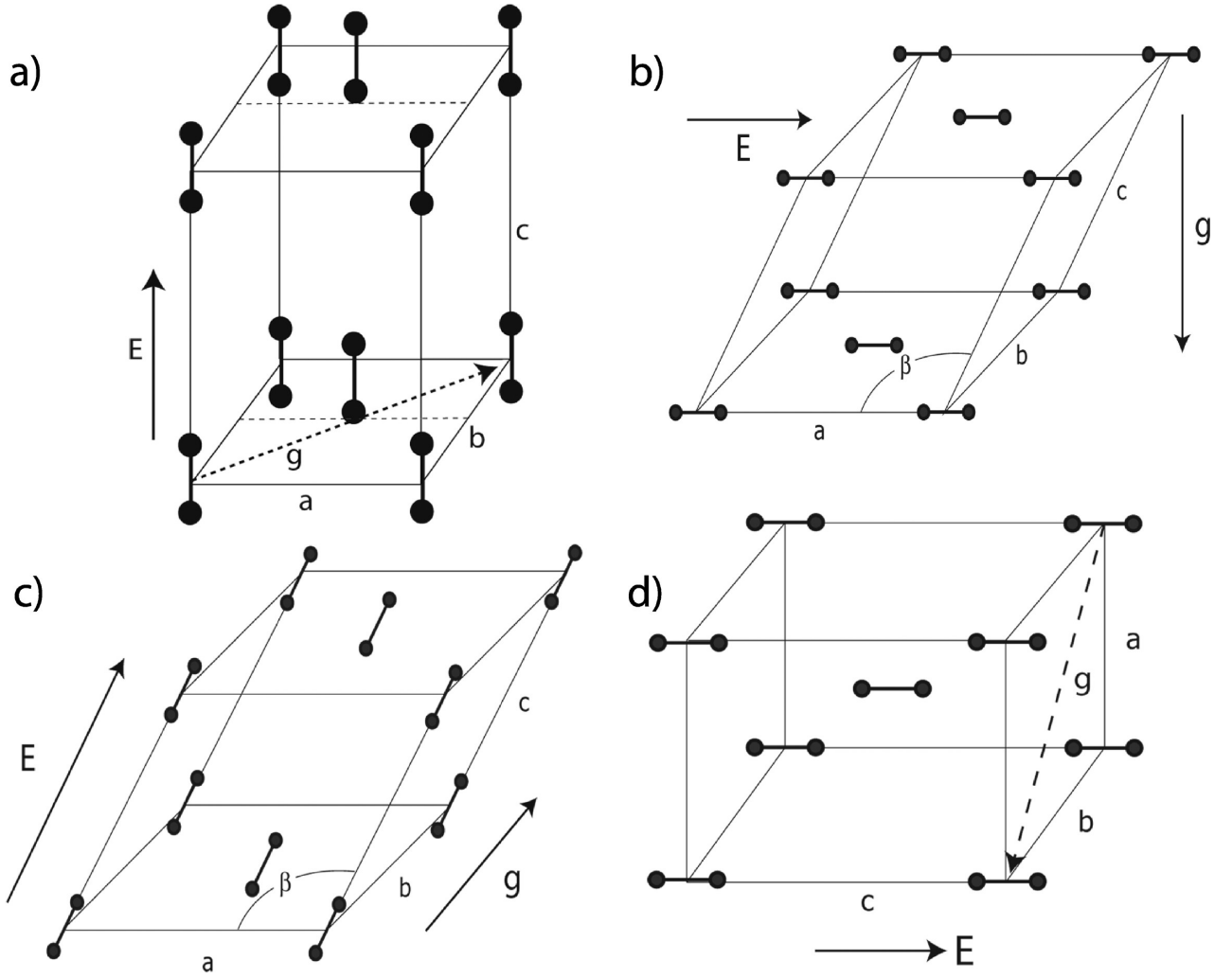

Figure 1. Unit cells for various structures observed. (a) Tetragonal unit cell of 0.9 aspect ratio hard dumbbell crystals formed in an electric field of 28 V_{rms}/mm. The crystal has a *P*4/*nmm* symmetry with space group number 129. (b) Base-centered monoclinic phase observed for 0.7 aspect ratio hard dumbbells in a field of 23 V_{rms}/mm and for 0.44 aspect ratio (effective) soft dumbbells in a field of 78 V_{rms}/mm. (c) Base-centered monoclinic phase observed less frequently for 0.44 aspect ratio soft dumbbells. (d) Body-centered-tetragonal (bct) phase observed for 0.7 hard dumbbells and 0.44 aspect ratio soft dumbbells at higher electric fields (37 V_{rms}/mm and 147 V_{rms}/mm for hard and soft dumbbells, respectively). "E" stands for the electric field and "g" for the direction of gravity.

Table 1. Crystal Structures of Dumbbells with Different Aspect Ratios, Interactions, and Electric Field Strengths

sample[a]	E-field	γ	space group	H-M symbol	Wyckhoff-β	parameters/μm	figure
0.9-hard-high	28 V_{rms}/mm	10.2	129[b]	*P*4/*nmm*	$c, z = -0.125$	$a = 1.5, b = 1.5, c = 2.45$	3b−d
0.7-hard-low	23 V_{rms}/mm	4.0	12[c]	*C*2/*m*	$a, \beta = 153°$	$a = 4.4, b = 1.7, c = 1.5$	4a−d
0.7-hard-high	37 V_{rms}/mm	10.3	139[d]	*I*4/*mmm*	*a*	$a = 1.1, b = 1.1, c = 4.1$	4e−h
0.4-soft-low-1	78 V_{rms}/mm	2.1	12[c]	*C*2/*m*	$a, \beta = 152°$	$a = 7.1, b = 3.2, c = 3.0$	5a−c
0.4-soft-low-2	78 V_{rms}/mm	2.1	12[c]	*C*2/*m*	$a, \beta = 136°$	$a = 3.0, b = 3.0, c = 4.0$	5d−f
0.6-soft-high	147 V_{rms}/mm	7.4	139[d]	*I*4/*mmm*	*a*	$a = 2.1, b = 2.1, c = 6.9$	5g−j

[a] The sample is described by aspect ratio, interaction, and field strength, respectively. [b] Tetragonal. [c] Monoclinic. [d] Body-centered-tetragonal.

for 0.7 aspect ratio. For 0.9 aspect ratio hard dumbbells, a lower γ experiment was not made due to lack of sample. For soft dumbbells, 0.9 aspect ratio particles were investigated at an effective aspect ratio of around 0.4 at γ of 2.1 (78 V_{rms}/mm), and this effective aspect ratio became 0.6 at γ of 7.4 (147 V_{rms}/mm). Effective aspect ratios were determined from confocal microscopy images by assuming the distance between the aligned dumbbells as σ and the distance between the dumbbell cores to be *L*. For finding the core locations, we used image processing language package IDL (RSI) and methods similar to those described by van Blaaderen et al.[4,8]

The symmetry of the crystal structures obtained for dumbbells was investigated with a computer program (*FINDSYM*) available online.[29]

3. Results and Discussion

Figure 1 and Table 1 summarize the crystal structures observed and the conditions probed. A tetragonal crystal (Figure 1a) and bct structures (Figure 1d) were observed for high electric fields, while base-centered-monoclinic (bcm) structures were observed for low electric fields (Figure 1b,c). As seen in Table 1, a variety of space groups, Wyckhoff positions,[30] and unit cell parameters

(29) Stokes, H. T.; Hatch, D. M. Online version of the FINDSYM programme available at http://stokes.byu.edu/findsym.html.

(30) *International Tables for Crystallography, Volume A Space Group Symmetry*, 5th ed., Hanh, Th., Ed.; 2005.

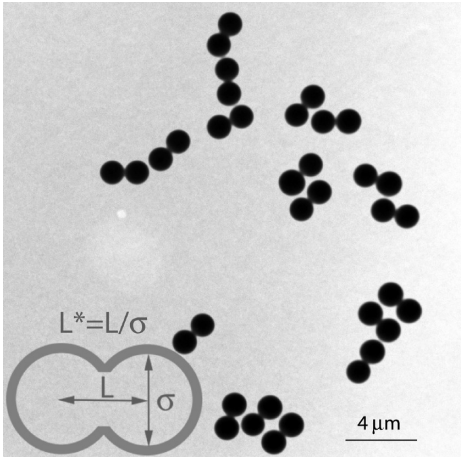

Figure 2. TEM image of 0.9 aspect ratio dumbbell particles. Inset shows the definition of the aspect ratio (L*).

were observed as a function of the aspect ratio, the interaction potential (hard or soft), and the electric field strength. The parameter γ, a dimensionless prefactor that measures the strength of the dipolar interactions, is also given in this table (see Experimental Section for an exact definition of γ). As we shall now describe, these six experimental cases provide a rich variety of structures and behaviors. Some of the structures can be compared and contrasted with colloid theory and with diatomic molecular crystals, while other results are unique to this system.

Figure 2 shows a TEM image of dumbbell particles used in this work. Here, the particles have an aspect ratio of 0.9. The inset in the figure depicts the definition of the aspect ratio (L*). Here, the aspect ratio of the particles is simply lowered by coating the particles with an extra layer of silica.

With no electric field applied, the bulk of the sediments formed glassy solids as illustrated in Figure 3a.[31] Confocal microscopy images of the crystals formed at high fields for hard 0.9 aspect ratio particles (0.9-hard-high) are shown in Figure 3b−d (Supporting Information Movie 1 of a 3D stack). The confocal stack is presented in several different orientations. The *xy*-plane given in Figure 3b shows the hexagonal ordering of the fluorescent cores. An overlay of images in the *xy*-plane from four different layers results in the image shown in Figure 3c. This image is similar to what one would observe for the bct structure of single spheres and shows the bridge-site stacking along the *y*-axis.[24] Figure 3d shows an image of the same stack of particles in the *xz*-plane. This clearly illustrates the **aba** stacking of the crystal and agrees with the designated tetragonal structure. Note that a single fluorescent core appears stretched in the *z*-direction due to the larger width of the microscope's point spread function in this direction.

Full coordinate analysis yielded a tetragonal structure with *P*4/*nmm* symmetry. As is seen from the unit cell given in Figure 1a, the dumbbells are aligned along the field direction and the dumbbells at the base centers are shifted by a quarter of a unit cell parameter in the field direction.

Confocal microscopy images of the crystals formed at low fields for hard 0.7 aspect ratio particles (0.7-hard-low) are shown in Figure 4a−d (see also Supporting Information Movie 2). As is seen in Figure 4a, the dumbbells can be easily distinguished as a result of the lower aspect ratio. The *xy* cross section in Figure 4a shows hexagonal ordering of the dumbbells. The **abcdea** stacking of the *xy*-layers is shown in Figure 4b. As in an fcc crystal, the identical hexagonal layers are shifted along the dumbbell length in the *y* direction. However, fcc shows **abca** stacking. Note also in this image that the cores from the left side of each dumbbell in the first and sixth layers are aligned with the right core in the fourth layer. This is consistent with the *xz* cut shown in Figure 4c in which only the **ada** layers are observed. Figure 4d shows an overlay of images in the *xy*-plane from eight different layers. This superposition resulted in a surprisingly sharp image, in which all holes are filled with the fluorescent cores forming regular hexagons. An fcc crystal of singles would yield a similar superposition. Thus, this arrangement appears to be close packing. In contrast to spheres, the close packing and stacking is aspect ratio specific.

Particle coordinate analysis showed the crystal structure to be bcm with the space group *C*2/*m*. The unit cell is shown in Figure 1b. It is notable that Vega et al.[32] predicted a bcm phase for hard dumbbells, which they named CP1 and CP2 for close-packed fcc-like and hcp-like stacking of the dumbbells. The consistency of the zero-field theory with our low field results suggests that the main effect of the external field is to align the particles. Induced dipole−dipole interactions appear to not dramatically affect the crystal structure.

At high electric field strengths, the dipole−dipole interactions become strong enough to affect the crystal structure. This occurred when the field was rapidly increased from 23 V_{rms}/mm (0.7-hard-low) to 37 V_{rms}/mm (0.7-hard-high). This higher field drove the structure into a bct phase in a few seconds. Given that the movements in the unit cell were small and did not require a restacking of layers this was a martensitic crystal−crystal transition.[33] Moreover, this martensitic transition was reversible.

Confocal microscopy images for the resulting phase are given in Figure 4e−h. The *xy*-plane, seen in Figure 4e, showed hexagonally ordered dumbbells, similar to the low field structure. However, the higher field altered the stacking along the *z*-axis. The *xy* layers were shifted half a period along the dumbbell length. This is visible in the image of the *yz*-plane given in Figure 4f. In this cross section, the third layer is aligned with the first, indicating **aba** stacking. Figure 4g is an image of the *xz*-plane showing a hexagonal arrangement of the fluorescent cores. Together, these observations indicate a bct phase (see Supporting Information Movie 3). A superposition of six consecutive layers parallel with the *xy*-plane resulted in the image given in Figure 4h, where bridge-site stacking of dumbbells along the *x*-axis, parallel to the dumbbell direction, is observed. The unit cell of this bct crystal is shown in Figure 1d.

Introducing soft interactions, resulting from the overlap of extended double layers around the charged particles through use of an organic solvent (CHB), created new, switchable structures.[9] As mentioned earlier, when no field was applied, a random plastic solid formed. When a field was applied, even to these sedimented structures, fully ordered crystals formed. These soft crystals were easier to obtain and to manipulate. Apparently, the increased separation between the particles due to the long-range interparticle repulsion provides enough rotational freedom for the particles to rearrange. This may explain the ordered crystals at lower γ (γ = 2.1) compared to the hard dumbbells.

Two different low-field soft crystal structures were observed, one of which (0.4-soft-low-1) was more prevalent than the other (0.4-soft-low-2). We will show that the two crystals share the same space group (*C*2/*m*) but have different unit cell parameters, stacking, and dumbbell orientations.

(31) Zhang, R.; Schweizer, K. S. *Phys. Rev. E* **2009**, *80*, 17.

(32) Vega, C.; Paras, E. P. A.; Monson, P. A. *J. Chem. Phys.* **1992**, *96*, 9060–9072.

(33) Yethiraj, A.; Wouterse, A.; Groh, B.; van Blaaderen, A. *Phys. Rev. Lett.* **2004**, *92*, 058301.

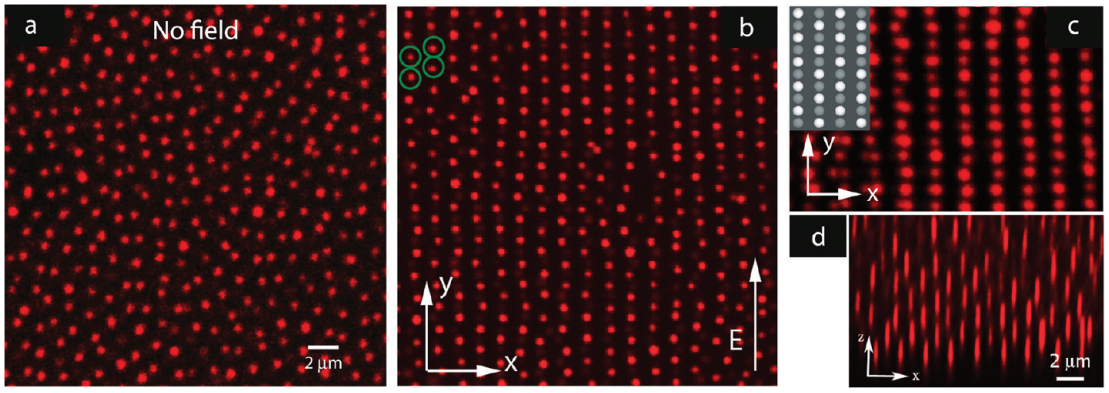

Figure 3. Confocal microscopy image of RITC labeled hard silica dumbbells. (a) Glass formed by sedimentation without an electric field. The aspect ratio of these particles is 0.7. (b) Image in the *xy*-plane of the 3D crystal stack (0.9-hard-high) formed in an electric field of 28 V_{rms}/mm with an aspect ratio of 0.9. Only fluorescent sphere centers of the dumbbells are visible; two full dumbbells are sketched. (c) Multilayer image of the same stack in the *xy*-plane with four layers of the stack superimposed. The inset shows a cartoon of two hexagonal planes of dumbbells overlaid, shown in white and gray, respectively. This demonstrates bridge-site stacking of the crystal. (d) *xz* scan of the same crystal where **aba** stacking is observed. Image sizes: (a) 23.3 μm × 23.3 μm, (b) 23.8 μm × 23.8 μm, (c) 21.6 μm × 13.2 μm, (d) 25.5 μm × ~8.5 μm.

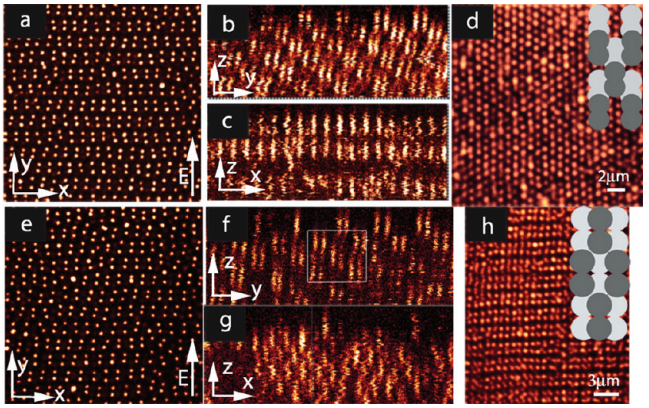

Figure 4. Confocal microscopy images of 0.7 aspect ratio hard dumbbell crystals at an electric field of 23 V_{rms}/mm (0.7-hard-low) (a−d) and 37 V_{rms}/mm (0.7-hard-high) (e−h). (a) Image of an *xy*-plane, where the dumbbells are oriented along the field and form a hexagonal pattern. (b) Image reconstructed from the same *z*-stack in the *zy*-plane where the **abcdea** stacking is observed. (c) Reconstructed image in the *xz*-plane where only the **ada** layers are visible. (d) Image made by projecting eight layers in the *xy*-plane, which is evidence for close-packing and the regularity of the crystal. The inset is a cartoon of the stacking of the hexagonal layers, where white and gray dumbbells show different layers. Image size (a) 27.1 μm × 27.1 μm. (e) Image in the *xy*-plane after the field is increased to 37 V_{rms}/mm. (f) An image in the *yz*-plane, reconstructed from the *z*-stack, where the **aba** stacking is shown. (g) An image in the *xz*-plane, reconstructed from the *z*-stack, where **aba** layers are visible. (h) Six layers of the *z*-stack are superimposed on each other showing the bridge-site stacking. Image size (e) 25.1 μm × 25.1 μm.

Confocal microscopy images of crystal 0.4-soft-low-1 are shown in Figure 5a−c. The slice of the *xy*-plane given in Figure 5a shows particles aligned along the field. Figure 5b shows **abca** stacking. The superposition of three layers in the *xz*-plane of the stack shown in Figure 5c shows the hexagonal ordering of the fluorescent cores (Supporting Information Movie 4).

Confocal microscopy images of crystal 0.4-soft-low-2 are shown in Figure 5d−f. As is seen from the *xy* cut in Figure 5d, particles were aligned head-to-toe parallel to the electric field, contrary to all other structures. This figure shows the particles forming parallelograms, not hexagons. The stacking shown in Figure 5e is **aba** where only **a** layers are visible (Supporting Information Movie 5). A projection of four layers in the *xy*-plane gave Figure 5f. In Figure 5f, two crystal domains were observed on the right and left with a line defect in the center.

Our coordinate analysis yielded *C*2/*m* symmetry for the low-field soft crystals, identical to the low-field hard dumbbells (0.7-hard-low). Apparently, the increased interparticle repulsion did not affect the crystal symmetry.

The unit cell angles β are 152° and 136° for 0.4-soft-low-1 and 0.4-soft-low-2, respectively. The unit cells of these phases are depicted in Figure 1b and c, respectively. Thus, 0.4-soft-low-1 shows an identical unit cell to 0.7-hard-low, while for 0.4-soft-low-2, the particles are aligned with the *c* axis. This result suggests that the more frequent 0.4-soft-low-1 domains grew from the *ab*-plane (the hexagonal plane), while the infrequent 0.4-soft-low-2 crystal domains grew from the *ac*-plane. These two phases coexist, and their relative fractions of these phases do not change in time. Subsequently, these orientations are affected differently by gravity and the electric field.

As the field strength was increased from 78 V_{rms}/mm to 147 V_{rms}/mm (raising γ to 7.4), another martensitic transition occurred. The soft crystal structure evolved to a bct phase (see Figure 1d for the unit cell). The high field increased the effective aspect ratio of the dumbbells in this crystal structure to 0.6. The confocal images given in Figure 5g−j show different planes of the structure (Supporting Information Movie 6). These images can be compared in all respects to the 0.7-hard-high case (Figure 4e−h). The coordinate analysis gives identical results to the 0.7-hard-high crystals except that the unit cell is larger for 0.6-soft-high.

It is interesting to compare our structures with crystals of diatomic molecules. The soft low-field crystals are perhaps best compared with α-O_2 and F_2, because they have similar aspect ratios (0.42 for α-O_2 and 0.50 for F_2). Furthermore, F_2 is thought to be a simple van der Waals solid with low quadrupolar interactions.[34] These molecular crystals indeed show the same bcm structure and *C*2/*m* symmetry as our low field colloidal crystals. The 0.7-hard-low crystal is most comparable in aspect ratio to Br_2, which has an aspect ratio of 0.72. However, Br_2 forms an orthorhombic crystal with *Cmca* symmetry.[34] This difference in structure can be explained by the presence of strong quadrupolar interactions in Br_2 that are not present in our colloidal dumbbells. Such interactions are thought to stabilize the orthorhombic phase of Br_2 with respect to the bcm phase.

(34) English, C. A.; Venables, J. A. *Proc. R. Soc. London, Ser. A* **1974**, *340*, 57–80.

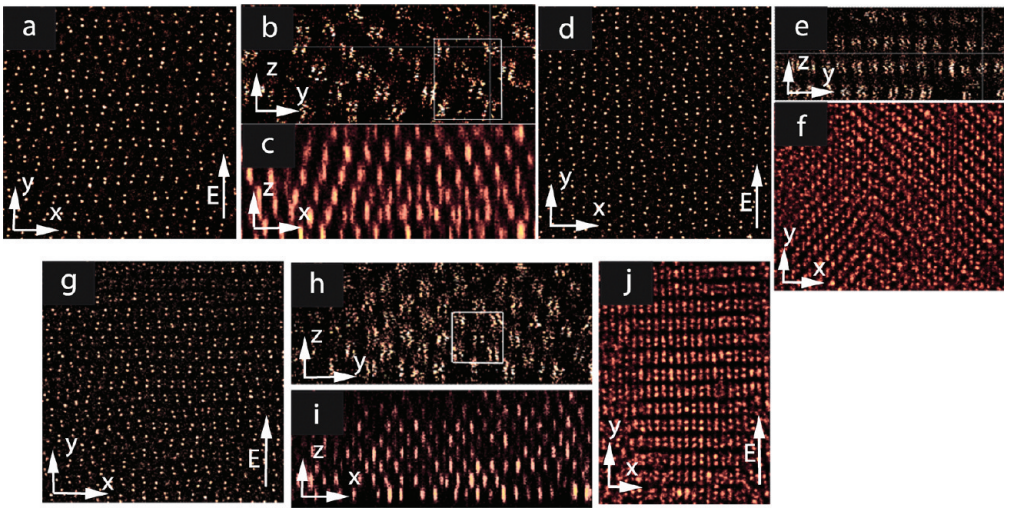

Figure 5. Confocal microscopy images of soft dumbbell crystals at an electric field of 78 V_{rms}/mm (a−f) and 147 V_{rms}/mm (g−j). Two kinds of bcm phases are observed at low fields: a−c (0.4-soft-low-1) is the frequently observed; d−f (0.4-soft-low-2) is the infrequent phase. (a) Image of the 0.4-soft-low-1 in the *xy*-plane. (b) Image in the *yz*-plane reconstructed from the 3D stack. The rectangular region outlines the **abca** stacking of the crystal. (c) Image in the *xz*-plane superimposed over three layers in this plane that shows the hexagonal order of the fluorescent cores of the dumbbells aligned along the field. Image size (a) = 46.8 μm × 46.8 μm. (d) Image of the 0.4-soft-low-2 in the *xy*-plane. (e) Image in the *yz*-plane reconstructed from the 3D stack. The **aa** layers of the **aba** stacking is seen, where **b** is not visible. (f) Overlay of four *xy* layers, which shows the **aba** stacking clearly. Image size (d) 55.3 μm × 55.3 μm. (g−j) Images of soft dumbbells, which form a bct crystal at an electric field of 147 V_{rms}/mm (0.6-soft-high). (g) Image of an *xy*-plane. (h) Image of an *yz*-plane reconstructed from the *z*-stack; the square region outlines the **aba** stacking of the crystal. (i) *xz*-scan of the stack showing the hexagonal order of the dumbbells aligned along the field. (j) Projection of six layers in the *xy*-plane, showing bridge-site stacking. Image size (g) 59.1 μm × 59.1 μm.

Comparing the unit cell angle β, we see that α-O_2 and F_2 have similar values (132° and 134.6°) to 0.4-soft-low-2 (β = 136°) but vary from the value for 0.7-hard-low and 0.4-soft-low-1 (β = 153° and 152°, respectively). For the 0.7-hard-low case, the difference can be explained by the differing aspect ratios. For the 0.4-soft-low-1 case, the difference may be attributed to the tendency of the colloidal particles to align with the field and gravity. Angle β is the angle between the unit cell vectors in a plane parallel to gravity. Compression of this plane makes β larger. In the unit cell, 0.4-soft-low-2 angle β depends only on particle shape and not on gravity.

Note that, as far as we know, there exist no comparable structures in molecular dimer crystals to our high field colloidal dumbbell crystals. This highlights the fact that the strong dipole−dipole interactions induced by the external field are quite different from the interactions of molecular dimers.

4. Conclusion

A number of conclusions can be summarized. The combination of anisotropic particles, soft interactions, and electric field increases the potential for finding new crystal structures strongly. We observed a remarkable diversity of structures, even with our relatively sparse sampling. Low electric fields aligned the dumbbells, preventing glass formation. The low field results are consistent with zero field literature predictions, both for colloidal dumbbells[32] and for certain molecular dimers. High fields drove martensitic transitions to new *I*4/*mmm* crystal structures. There are no theories available for the high-field crystals yet. Moreover, the soft interactions facilitated crystallization and enabled the manipulation of the crystal properties with an electric field. For these systems, the electric field could be used to reorient the dumbbells while maintaining crystallinity. It was also possible to restructure the crystal by turning the electric field on and off. Such switching behavior is interesting for photonic use of these crystals.

A more extensive study of the phase behavior, possible martensitic switching, and the glass formations in these systems is warranted. It would also be interesting to explore a similar dispersion in a density-matched system. This would allow more detailed exploration of zero field case. Finally, a detailed theory for the high-field case is warranted.

Acknowledgment. The authors thank Hanumantha Rao Vutukuri and Johan C. P. Stiefelhagen for helpful discussions. Part of this research was supported by the EU (NanoDirect, grant number CP-FP-213948-2). P.D.J. was part of the research program of the Stichting voor Fundamenteel Onderzoek der Materie, which is financially supported by the Nederlandse Organisatie voor Wetenschappelijk Onderzoek.

Supporting Information Available: Movies that were constructed from confocal microscopy images scanned through the crystal in the *z*-axis are given for the following systems: 0.9-hard-high (Movie 1), 0.7-hard-low (Movie 2), 0.7-hard-high (Movie 3), 0.4-soft-low-1 (Movie 4), 0.4-soft-low-2 (Movie 5), 0.6-soft-high (Movie 6). This material is available free of charge via the Internet at http://pubs.acs.org.